1

Supplemental Material for

2

3

The influence of summer deep soil temperature on early winter snow conditions in Eurasia in the NCEP CFSv2 simulation

6

Ravi P. Shukla[1,*], Bohua Huang[1,2], Paul A Dirmeyer[1,2] and James L. Kinter[1,2]

[1]Center for Ocean-Land-Atmosphere Studies
George Mason University, Fairfax, Virginia, USA

[2]Department of Atmospheric, Oceanic, and Earth Sciences, George Mason University, Fairfax, Virginia, USA

Contents of this file: Figures S1 to S9

*Corresponding author:
Dr. Ravi P. Shukla
Center for Ocean-Land-Atmosphere Studies (COLA)
George Mason University
270 Research Hall, Mail Stop 6C5, ,
4400 University Drive, Fairfax, VA 22030 USA
E-mail: rshukla2@gmu.edu

Supplementary Figures:

Figure S1. Spatial distribution of the climatological observed SCF [%] in **(a)** Sep, **(b)** Oct, **(c)** Nov and **(d)** Dec. The scale for the magnitude of SCF in "%" is shown below these panels (1st). **(e)-(h)** as in (a)-(d) but for SWE [kg/m^2]. The scale for the magnitude of SWE in "kg/m^2" is shown at below these panels (2nd). **(i)-(l)** as in (a)-(d) but for Surface Albedo (SA). The scale for the magnitude of bias for Surface Albedo in "%" is shown at right of these panels.

Figure S2. Spatial distribution of the climatological CFSR reanalysis 2-meter Temperature (T2m) [degree Kelvin; $^{\circ}K$] in **(a)** SON, **(b)** DJF, **(c)** MAM and **(d)** JJA. The scale for the magnitude for 2-m Temperature in "$^{\circ}K$" is shown at left of these panels. Spatial distributions of seasonal mean T2m biases relative to CFSR in model simulation for **(e)** JJA, **(f)** SON, **(g)** DJF and **(h)** MAM. The scale for the magnitude of bias for surface temperature in "$^{\circ}K$" is shown right of these panels.

Figure S3. Spatial distribution of the climatological ERA40 reanalysis land surface temperature (LST) [degree Kelvin; $^{\circ}K$] in **(a)** SON, **(b)** DJF, **(c)** MAM and **(d)** JJA. The scale for the magnitude for LST in "$^{\circ}K$" is shown at left of these panels. Spatial distributions of seasonal mean LST biases relative to ERA40 in model simulation for **(e)** JJA, **(f)** SON, **(g)** DJF and **(h)** MAM. The scale for the magnitude of bias for surface temperature in "$^{\circ}K$" is shown right of these panels.

Figure S4. Spatial distribution of the monthly climatological ERA40 LST [$^{\circ}K$] in **(a)** Jul, **(b)** Aug, **(c)** Sep, **(d)** Oct and **(e)** Nov. The scale for the magnitude for LST in "K" is shown at left of these panels. Spatial distributions of the monthly climatological LST bias relative to ERA40 in model simulation for **(f)** Jul, **(g)** Aug, **(h)** Sep, **(i)** Oct and **(j)** Nov. The scale for the magnitude of bias for LST in "$^{\circ}K$" is shown at right of these panels. Both red and pink lines in all the panels depict 273.15 $^{\circ}K$ (freezing temperature) for ERA40 (red line) and CFSv2 (black line).

Figure S5. Spatial distribution of the climatological ERA40 reanalysis 2-meter Temperature (T2m) [degree Kelvin; $^{\circ}K$] in **(a)** SON, **(b)** DJF, **(c)** MAM and **(d)** JJA. The scale for the magnitude for LST in "$^{\circ}K$" is shown at left of these panels. Spatial distributions of seasonal mean T2m biases relative to ERA40 in model simulation for **(e)** JJA, **(f)** SON, **(g)** DJF and **(h)** MAM. The scale for the magnitude of bias for surface temperature in "$^{\circ}K$" is shown right of these panels.

Figure S6. Spatial distributions of the monthly climatological LST biases relative to CFSR in CFSv2 simulation for **(a)** Apr, **(b)** May and **(c)** Jun. Both red and pink lines in all the panels depict 273.15 ^{o}K (freezing temperature) for CFSR (red line) and CFSv2 simulation (black line). **(d)-(e)** as in (a)-(c) but for SUBT at 0-10cm. **(d)-(e)** as in (a)-(c) but for SUBT at 10-40cm. **(d)-(e)** as in (a)-(c) but for SUBT at 40-100cm. **(d)-(e)** as in (a)-(c) but for SUBT at 100-200cm.

Figure S7. Difference between mean of five cold years and warm years of SUBT at 100-200cm over the western Eurasian (outlined by black box in Figure S7; 42°N-64°N, 18°E-58°E) during July to September mean (JAS) in the CFSv2 simulation. **(b)** as in (a) SUBT at 0-10cm during October. The red line (black line) in Fig. S7(b) denotes 273.15^{o}K in cold year (warm year) in CFSv2. **(c)** as in (a) but for LST during October. The red line (black line) in Fig. S7(c) denotes 273.15^{o}K in cold year (warm year) in CFSv2. **(d)** as in (a) but for SCF during October. **(e)-(h)** as in (a)-(d) but for CFSR reanalysis respectively.

Figure S8. **(a-f)** Spatial distributions of monthly surface sensible heat flux climatological biases relative to observation in model simulation during May to October.   **(g-l)** as in (a-f) but for net LWR. The net LWR is defined as difference between downward LWR and upward LWR. **(m-r)** as in (a-f) but for net SWR. The net SWR is defined as difference between downward SWR and upward SWR.

Figure S9: Spatial distributions of monthly mean temperature (1000hPa to 600hPa; hereafter, MT) climatological biases relative to CFSR in model simulation for **(a)** April (Feb), **(b)** May (May), **(c)** June (Jun), **(d)** July (Jul), **(e)** September (Sep). and **(f)** October (Oct). The scale for the magnitude for MT bias in ^{o}K is shown below these panels. **(g-l)** as in (a-f) but for monthly H500 climatological bias relative to reanalysis in model simulation. The scale for the magnitude for H500 bias in meter is shown right of these panels (1st one). **(m-r)** as in (a-f) but for 500hPa-wind bias relative to reanalysis in model simulation. The scale for the magnitude for 500hPa-wind bias in meter/second is shown right of these panels (2nd one).
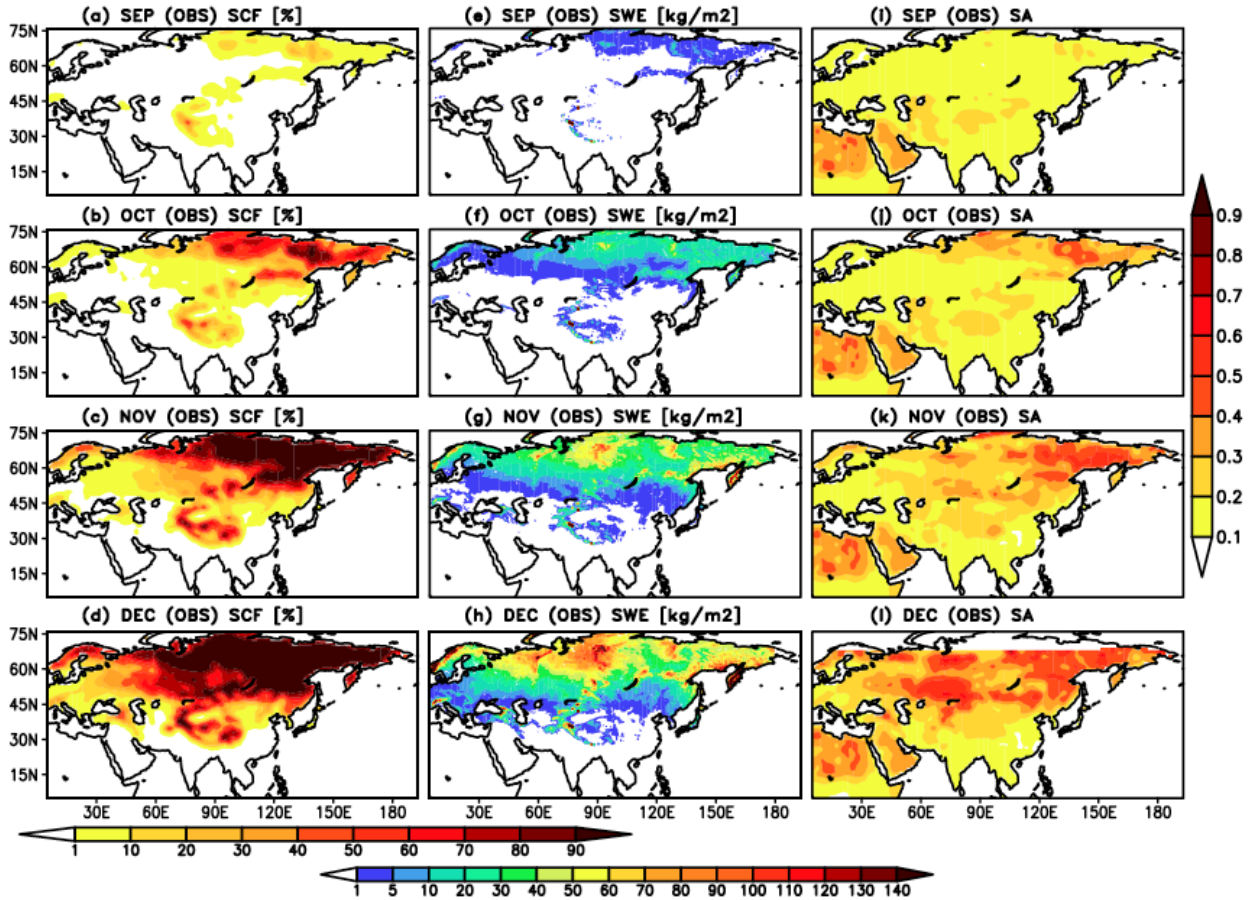
99
100
101
102
103

104

Figure S1. Spatial distribution of the climatological observed SCF [%] in **(a)** Sep, **(b)** Oct, **(c)** Nov and **(d)** Dec. The scale for the magnitude of SCF in "%" is shown below these panels (1st). **(e)-(h)** as in (a)-(d) but for SWE [kg/m^2]. The scale for the magnitude of SWE in "kg/m^2" is shown at below these panels (2nd). **(i)-(l)** as in (a)-(d) but for Surface Albedo (SA). The scale for the magnitude of bias for Surface Albedo in "%" is shown at right of these panels.

110

111

112

113

114

115

116
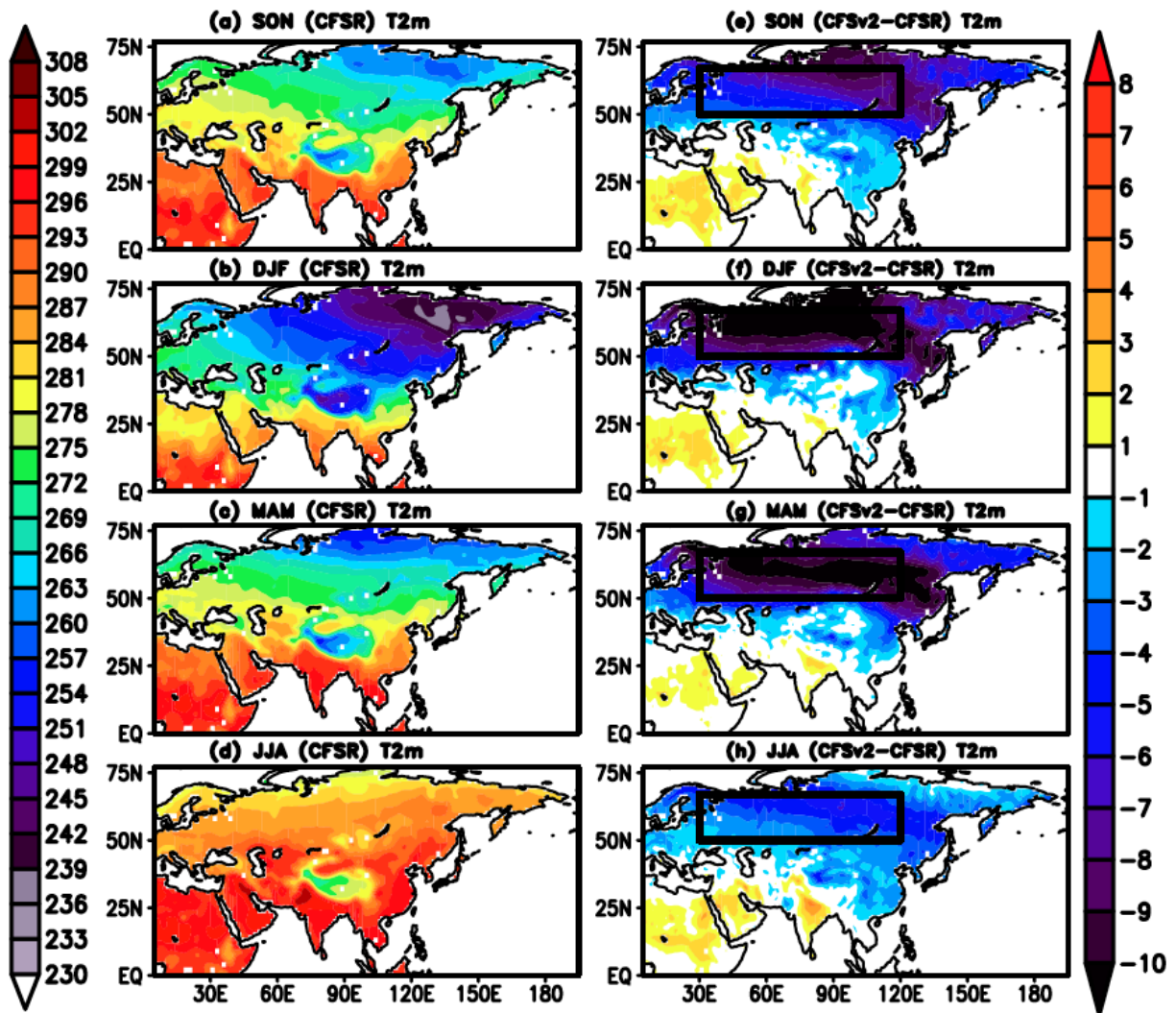
117

Figure S2. Spatial distribution of the climatological CFSR reanalysis 2-meter Temperature (T2m) [degree Kelvin; ^{o}K] in **(a)** SON, **(b)** DJF, **(c)** MAM and **(d)** JJA. The scale for the magnitude for 2-m Temperature in "^{o}K" is shown at left of these panels. Spatial distributions of seasonal mean T2m biases relative to CFSR in model simulation for **(e)** JJA, **(f)** SON, **(g)** DJF and **(h)** MAM. The scale for the magnitude of bias for surface temperature in "^{o}K" is shown right of these panels.
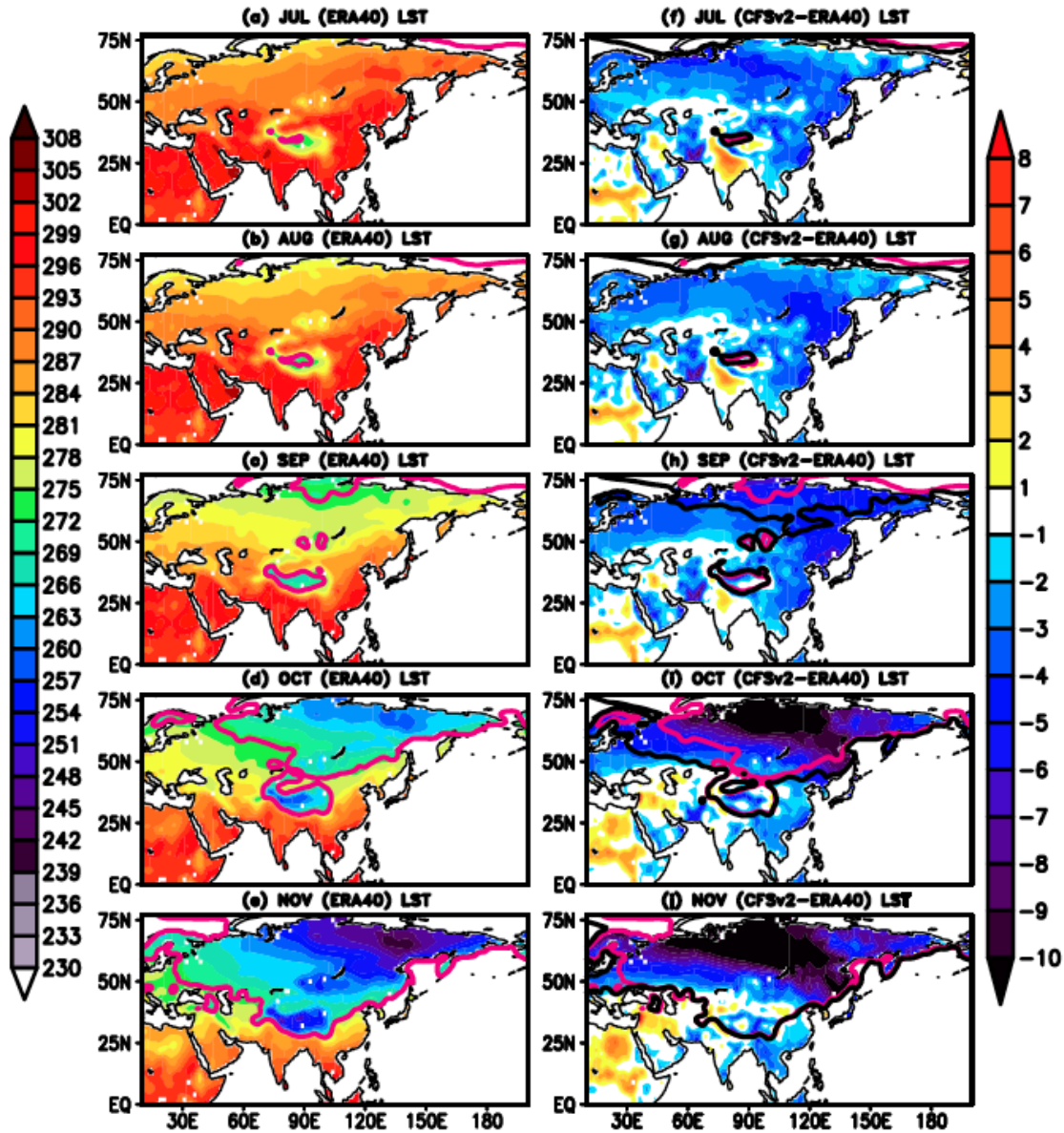
123
124
125
126
127

128

129

130
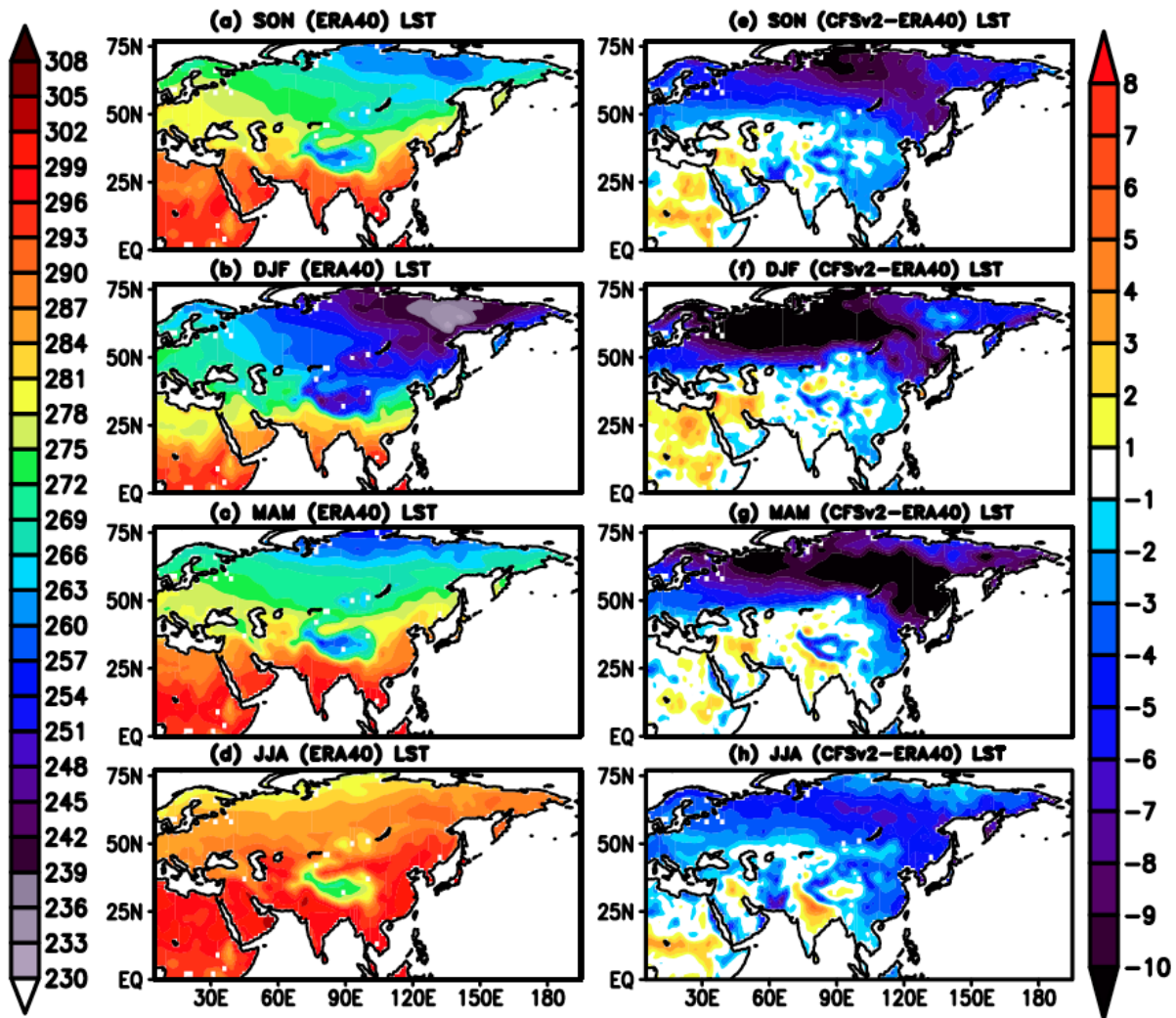
131

132 **Figure S3**. Spatial distribution of the climatological ERA40 reanalysis land surface temperature
133 (LST) [degree Kelvin; ºK] in **(a)** SON, **(b)** DJF, **(c)** MAM and **(d)** JJA. The scale for the magnitude
134 for LST in "ºK" is shown at left of these panels. Spatial distributions of seasonal mean LST biases
135 relative to ERA40 in model simulation for **(e)** JJA, **(f)** SON, **(g)** DJF and **(h)** MAM. The scale for
136 the magnitude of bias for surface temperature in "ºK" is shown right of these panels.
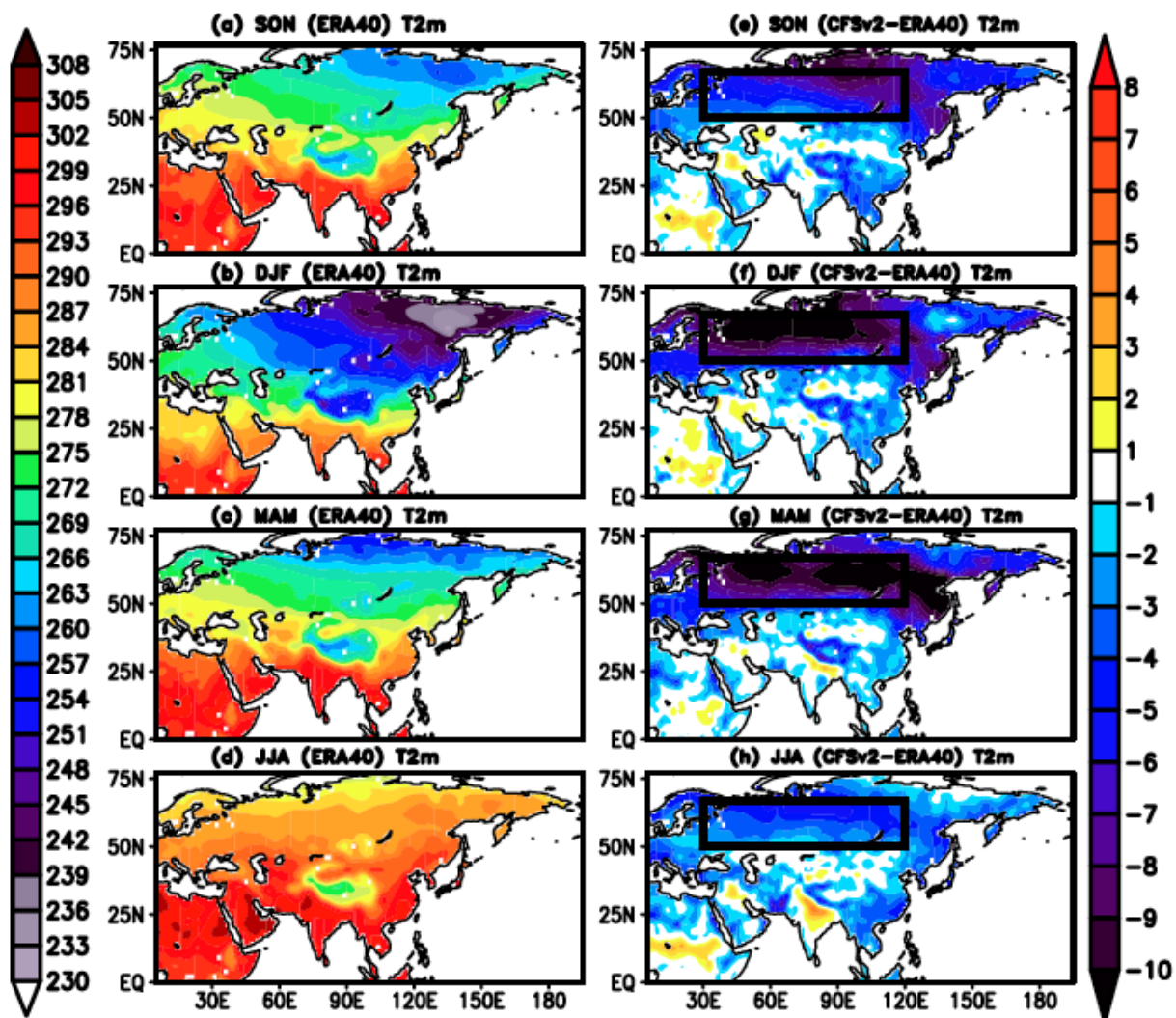
137

138

139

140

Figure S4. Spatial distribution of the monthly climatological ERA40 LST [ºK] in **(a)** Jul, **(b)** Aug, **(c)** Sep, **(d)** Oct and **(e)** Nov. The scale for the magnitude for LST in "K" is shown at left of these panels. Spatial distributions of the monthly climatological LST bias relative to ERA40 in model simulation for **(f)** Jul, **(g)** Aug, **(h)** Sep, **(i)** Oct and **(j)** Nov. The scale for the magnitude of bias for LST in ""ºK" is shown at right of these panels. Both red and pink lines in all the panels depict 273.15 ºK (freezing temperature) for ERA40 (red line) and CFSv2 (black line).

152

153

154 **Figure S5**. Spatial distribution of the climatological ERA40 reanalysis 2-meter Temperature (T2m)
155 [degree Kelvin; °K] in **(a)** SON, **(b)** DJF, **(c)** MAM and **(d)** JJA. The scale for the magnitude for
156 LST in ""°K" is shown at left of these panels. Spatial distributions of seasonal mean T2m biases
157 relative to ERA40 in model simulation for **(e)** JJA, **(f)** SON, **(g)** DJF and **(h)** MAM. The scale for
158 the magnitude of bias for surface temperature in ""°K" is shown right of these panels.

159

160
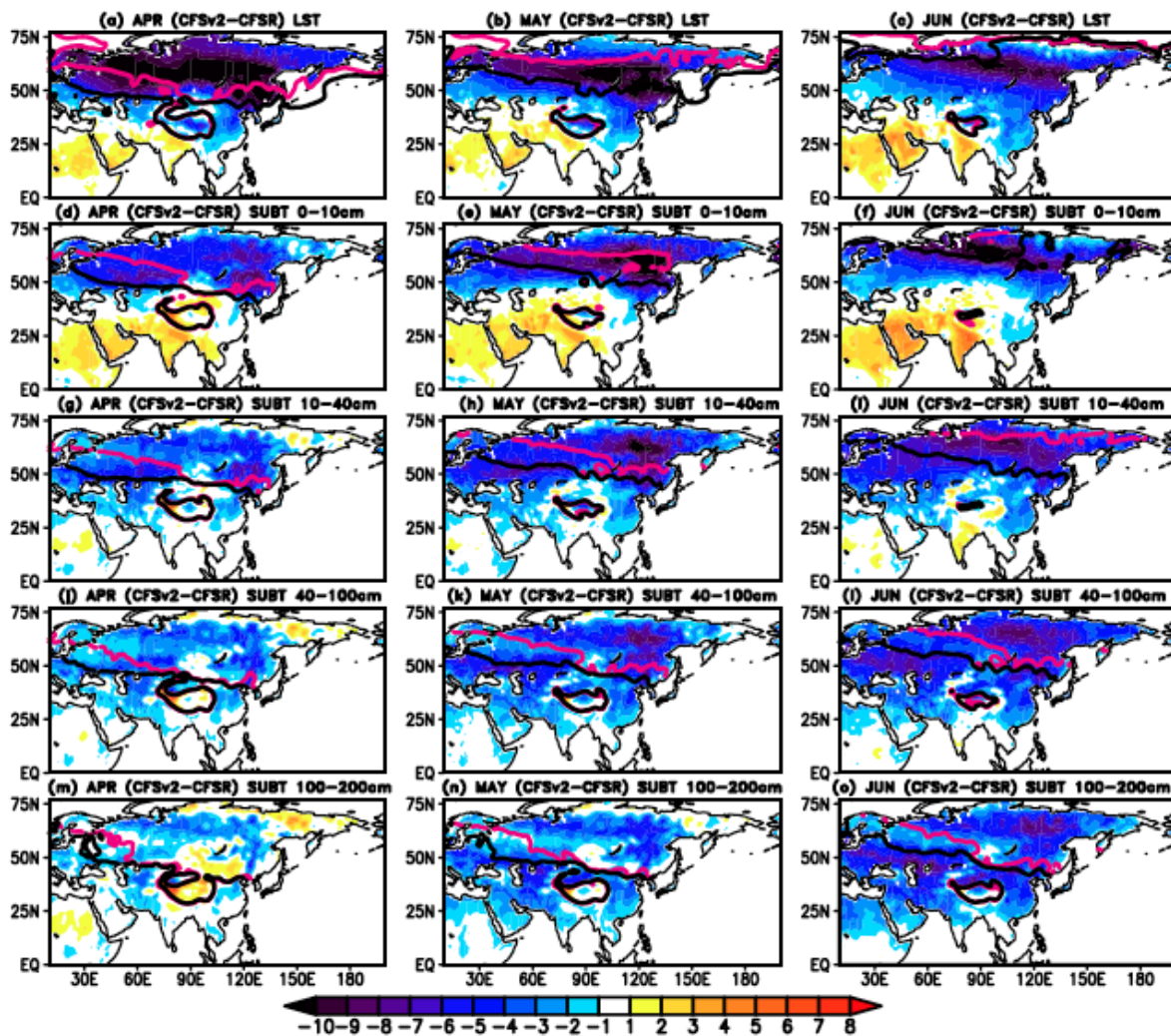
161

162

163

164

165

Figure S6. Spatial distributions of the monthly climatological LST biases relative to CFSR in CFSv2 simulation for **(a)** Apr, **(b)** May and **(c)** Jun. Both red and pink lines in all the panels depict 273.15 °K (freezing temperature) for CFSR (red line) and CFSv2 simulation (black line). **(d)-(e)** as in (a)-(c) but for SUBT at 0-10cm. **(d)-(e)** as in (a)-(c) but for SUBT at 10-40cm. **(d)-(e)** as in (a)-(c) but for SUBT at 40-100cm. **(d)-(e)** as in (a)-(c) but for SUBT at 100-200cm.
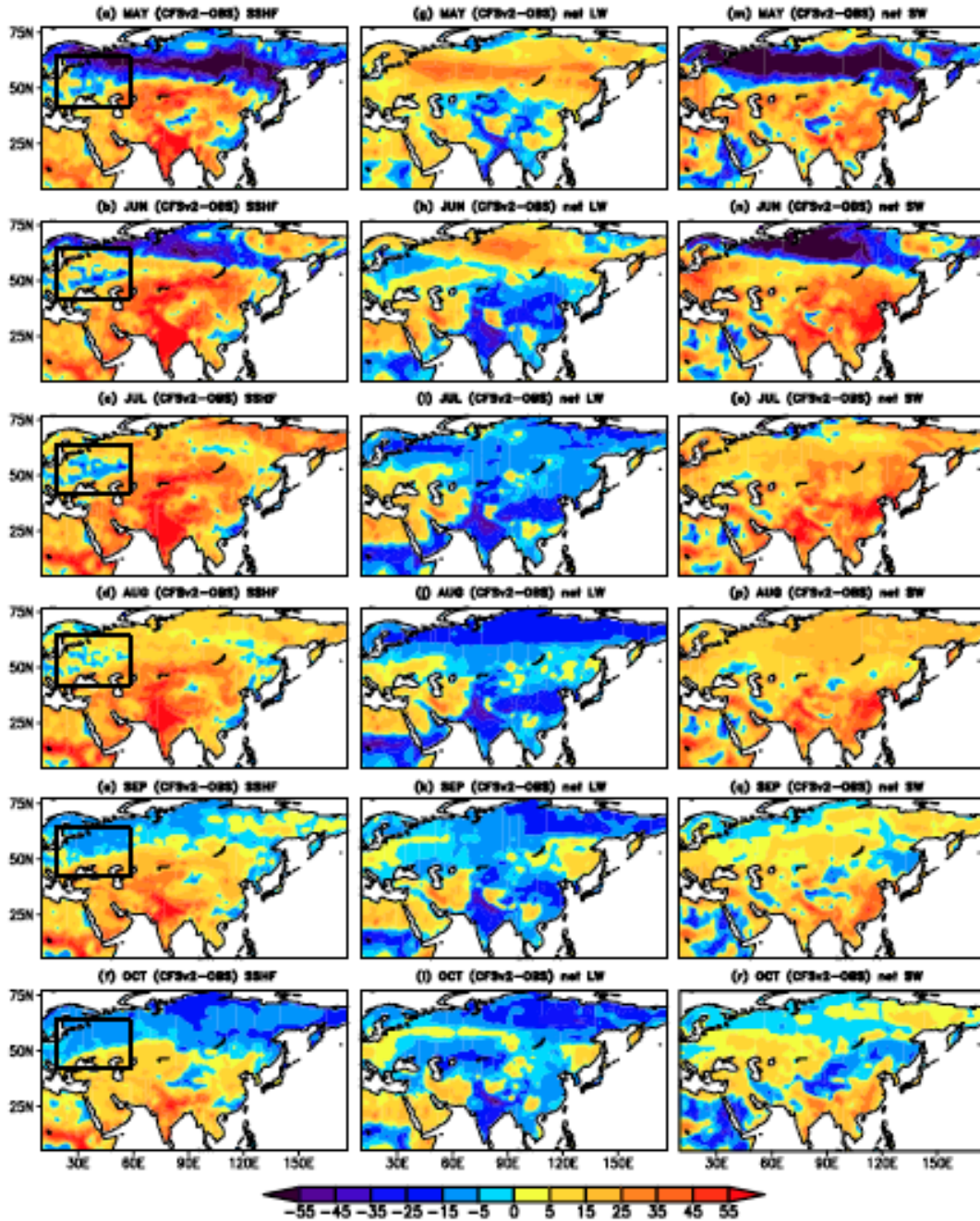
172

173

174

175
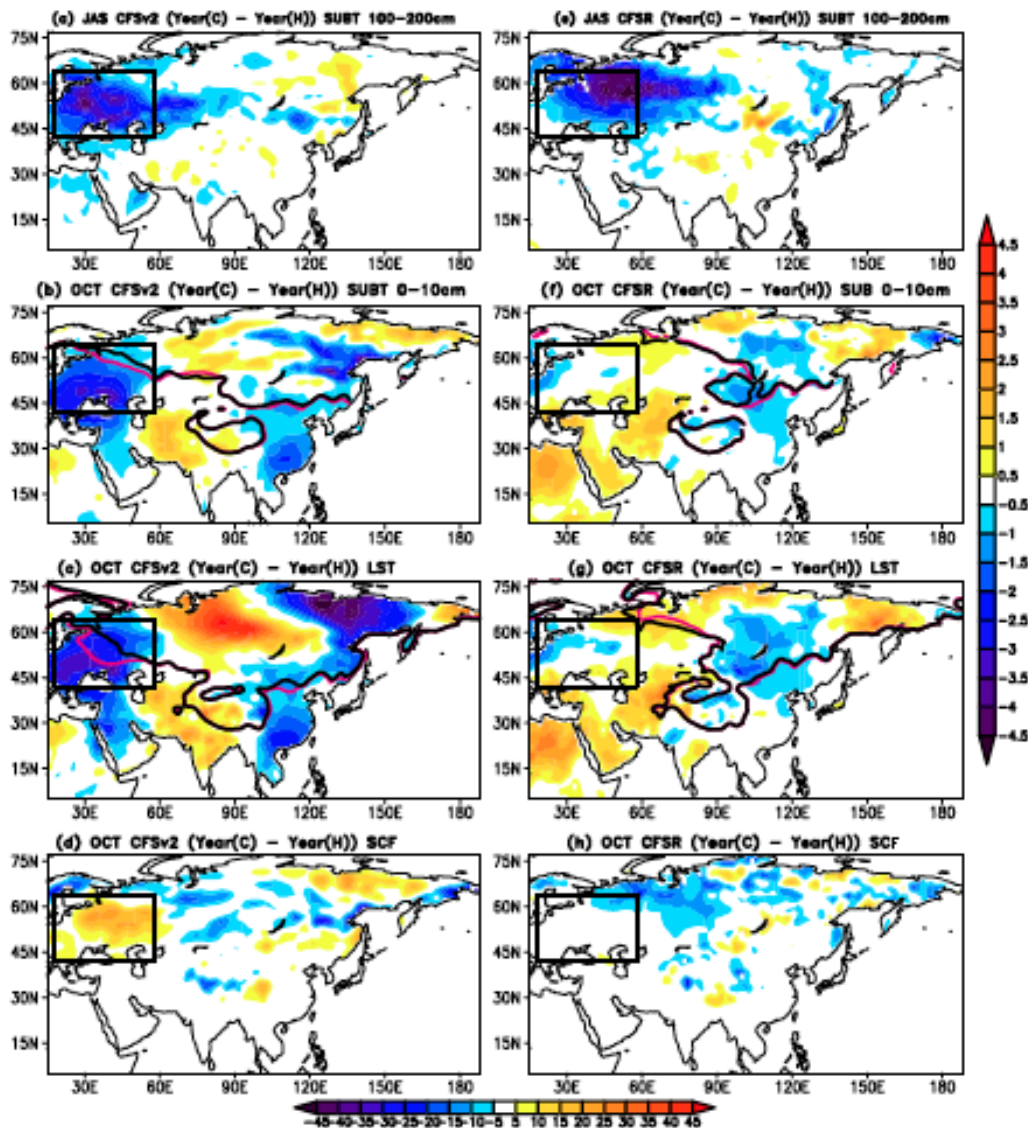
9

176

177

Figure S7. Difference between mean of five cold years and warm years of SUBT at 100-200cm over the western Eurasian (outlined by black box in Figure S7; 42ºN-64ºN, 18ºE-58ºE) during July to September mean (JAS) in the CFSv2 simulation. (**b**) as in (a) SUBT at 0-10cm during October. The red line (black line) in Fig. S7(b) denotes 273.15ºK in cold year (warm year) in CFSv2. (**c**) as in (a) but for LST during October. The red line (black line) in Fig. S7(c) denotes 273.15ºK in cold year (warm year) in CFSv2. (**d**) as in (a) but for SCF during October. (**e**)-(**h**) as in (a)-(d) but for CFSR reanalysis respectively.
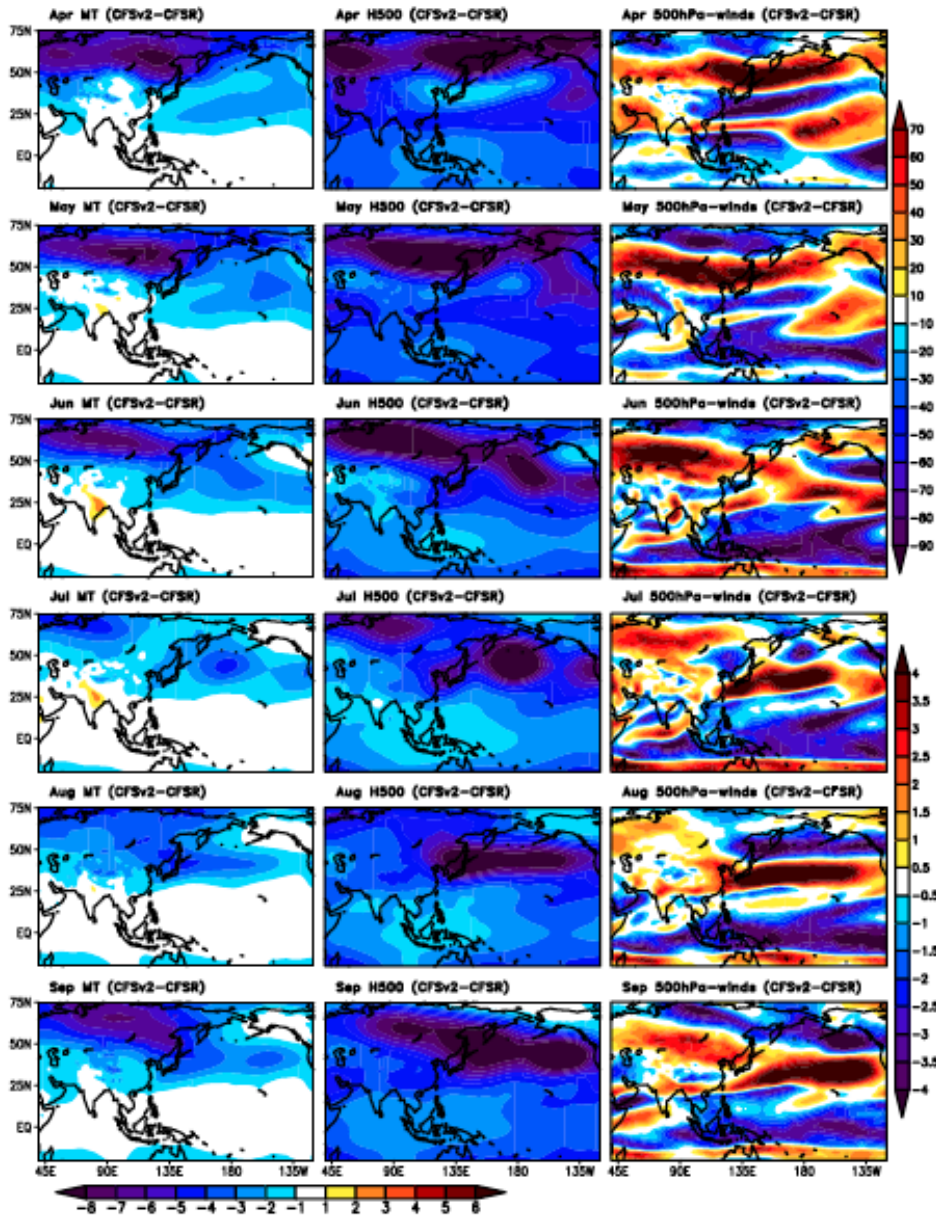
185

186

187

188

Figure S8. **(a-f)** Spatial distributions of monthly surface sensible heat flux climatological biases relative to observation in model simulation during May to October. **(g-l)** as in (a-f) but for net LWR. The net LWR is defined as difference between downward LWR and upward LWR. **(m-r)** as in (a-f) but for net SWR. The net SWR is defined as difference between downward SWR and upward SWR.

189
190
191
192
193
194

195

196

197

Figure S9: Spatial distributions of monthly mean temperature (1000hPa to 600hPa; hereafter, MT) climatological biases relative to CFSR in model simulation for **(a)** April (Feb), **(b)** May (May), **(c)** June (Jun), **(d)** July (Jul), **(e)** September (Sep). and **(f)** October (Oct). The scale for the magnitude for MT bias in °K is shown below these panels. **(g-l)** as in (a-f) but for monthly H500 climatological bias relative to reanalysis in model simulation. The scale for the magnitude for H500 bias in meter is shown right of these panels (1ˢᵗ one). **(m-r)** as in (a-f) but for 500hPa-wind bias relative to reanalysis in model simulation. The scale for the magnitude for 500hPa-wind bias in meter/second is shown right of these panels (2ⁿᵈ one).